

# Radiative recombination during ambipolar carrier transport by surface acoustic waves in GaAs quantum wells

S. K. Zhang, P. V. Santos,<sup>a)</sup> and R. Hey

Paul-Drude-Institut für Festkörperelektronik, Hausvogteiplatz 5–7, 10117 Berlin, Germany

(Received 6 November 2001; accepted for publication 25 January 2002)

We report on the defect-assisted radiative recombination of photogenerated electrons and holes in GaAs quantum wells (QWs) during the transport by surface acoustic waves (SAWs). The studies were performed by detecting the spatial distribution of the photoluminescence (PL) with a resolution of a few micrometers. Under a SAW, a high PL intensity is observed on spatially localized spots along the SAW propagation path. This high PL intensity is attributed to recombination of the carriers, which are transported by the SAW, induced by charged defects located on or close to the QW plane. © 2002 American Institute of Physics. [DOI: 10.1063/1.1463706]

A surface acoustic wave (SAW) traveling in a piezoelectric medium creates a piezoelectric potential  $\phi_{\text{SAW}}$  with the same temporal and spatial periodicities as the SAW acoustic field.<sup>1</sup> The potential  $\phi_{\text{SAW}}$  is sufficiently strong to trap and transport electrons ( $e$ ) or holes ( $h$ ) with the SAW velocity  $v_{\text{SAW}}$ . This SAW-driven transport has been proposed for applications in high-speed analog signal processing,<sup>2</sup> light modulators,<sup>3</sup> as well as for single-electron devices.<sup>4</sup> Recently, Rocke *et al.*<sup>5</sup> have demonstrated that the moving piezoelectric potential can also dissociate photogenerated excitons and trap the free  $e$  and  $h$  at its maxima and minima, respectively, thus leading to an ambipolar carrier transport. In addition, the spatial separation of the carriers leads to a remarkable increase of their recombination lifetimes. Since the SAW velocity is several orders of magnitude lower than the light speed, the storage of  $e$  and  $h$  in the SAW potential provides a practical way of realizing optical memory devices.

An important issue associated with the SAW-induced transport concerns the role of defects, which may distort the charge packets and reduce the transport efficiency.<sup>6,7</sup> In this work, we investigate the effect of defects on the SAW-induced ambipolar transport of  $e$  and  $h$  in GaAs quantum wells (QWs) using spatially resolved photoluminescence (PL). We demonstrate that the transport efficiency is limited by the radiative carrier recombination at sites located along the SAW propagation path. Interestingly, these sites do not significantly affect the normal diffusion of excitons, which takes place in the absence of a SAW. The recombination sites are attributed to charged defects in or close to the QW plane, which trap the carriers transported by the SAW, thus inducing their recombination.

The samples used in these studies consist of nominally undoped single GaAs QWs with  $\text{Al}_{0.3}\text{Ga}_{0.7}\text{As}$  barriers grown by molecular-beam epitaxy. The GaAs QW is 15 nm wide and located 200 nm below the surface. SAWs propagating along the  $[0\bar{1}1]$  direction on the (100) sample surface were generated using split-finger interdigital transducers (IDTs) designed for operation at a wavelength  $\lambda_{\text{SAW}}$  of 5.6  $\mu\text{m}$  (cor-

responding to a SAW frequency of 520 MHz at 15 K). Spatially resolved PL measurements were performed at that temperature using a microscope with adjustable illumination and detection areas, each with a diameter of approximately 2  $\mu\text{m}$ . The measurements were carried out on the SAW propagation path around an arbitrary reference position  $P_0 = (x=0, y=0)$   $\mu\text{m}$  located approximately 100  $\mu\text{m}$  away from the edge of the IDT, as shown in the inset of Fig. 1. The PL was excited using a cw radiation from a Ti-sapphire laser ( $\lambda_L = 750$  nm), which is transparent to the barriers.

The solid lines in Fig. 1 show typical PL spectra recorded for confocal illumination and detection at  $P_0$  in the absence (thin line) and in the presence of a SAW (thick line). In the absence of a SAW, the strong PL peak at 1.533 eV and the weak line at 1.539 eV are assigned to the electron-heavy-hole ( $e$ -hh) and to the electron-light-hole ( $e$ -lh) transitions in the QW, respectively. The  $e$ -hh line consists of two overlapping components with an energy separation of approximately 0.5 meV, which are attributed to a localized and to the free-exciton states, respectively. These two components become resolved in PL spectra recorded under a SAW [thick line in Fig. 1(b)]. The overlap between the two lines prevents a clear observation of the splitting of the tran-

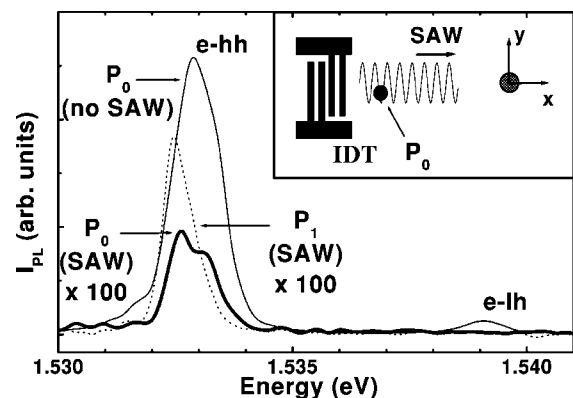


FIG. 1. Excitonic PL spectra recorded in the absence (thin line) and in the presence of a SAW (thick line) for confocal excitation and detection at the reference position  $P_0$ . The dotted line displays the PL spectrum detected under a SAW at the luminescence site  $P_1$ , for excitation at  $P_0$ . The inset shows a schematic setup of the PL measurements. The PL was excited by applying a nominal rf power of 13 dBm to the IDT.

<sup>a)</sup>Electronic mail: santos@pdi-berlin.de

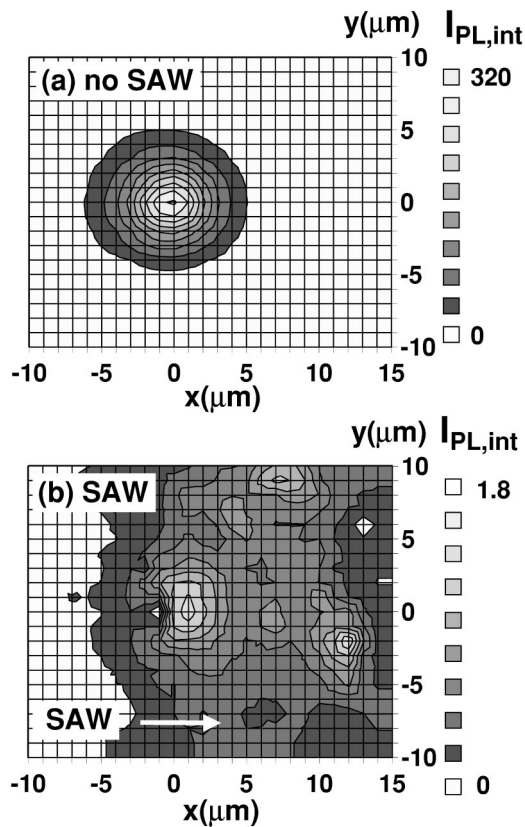


FIG. 2. Spatial distribution of the integrated PL intensity  $I_{PL,int}$  (arbitrary units, linear scale) (a) in the absence and (b) in the presence of a SAW (rf power of 13 dBm).

sition lines, which is expected due to the band-gap modulation induced by the SAW strain field.<sup>9</sup> In addition, the PL intensity becomes strongly suppressed as a consequence of the ionization of the photogenerated excitons and the subsequent transport of the free  $e$  and  $h$  away from the detection area by the moving SAW field.<sup>8,5,9</sup>

The SAW-induced ambipolar transport can be directly visualized by measuring the spatial distribution of the PL around a microscopic illumination spot. The contour plots in Figs. 2(a) and 2(b) show the spatial dependence of the integrated PL intensity  $I_{PL,int}$  around  $P_0$  in the absence and in the presence of a SAW, respectively.  $I_{PL,int}$  was obtained by integrating the PL spectrum over the energy range of the  $e-h$  transition (between 1.530 and 1.536 eV, cf. Fig. 1). The symmetric  $I_{PL,int}$  distribution in Fig. 2(a) is attributed to the isotropic exciton diffusion away from the generation area. In contrast, the distribution profile in Fig. 2(b) becomes asymmetric under a SAW due to the ambipolar carrier transport along the SAW propagation direction. Compared with Fig. 2(a), the spatial separation of  $e$  and  $h$  by the SAW piezoelectric field leads to an increased recombination lifetime and, thus, to much longer carrier diffusion lengths in the direction parallel to the SAW wave fronts ( $y$  direction).

A striking phenomenon in Fig. 2(b) is the appearance of spots of strong PL emission at positions far away from the generation area [e.g., at positions  $P_1=(12,-2)\mu\text{m}$ ,  $P_2=(7.5,9)\mu\text{m}$ , and  $P_3=(4,7)\mu\text{m}$ ]. The lateral extent of these luminescence sites (LSs) is smaller than the SAW wavelength. The PL spectrum recorded at position  $P_1$  for excitation at  $P_0$  is displayed by the dotted curve in Fig. 1. Note

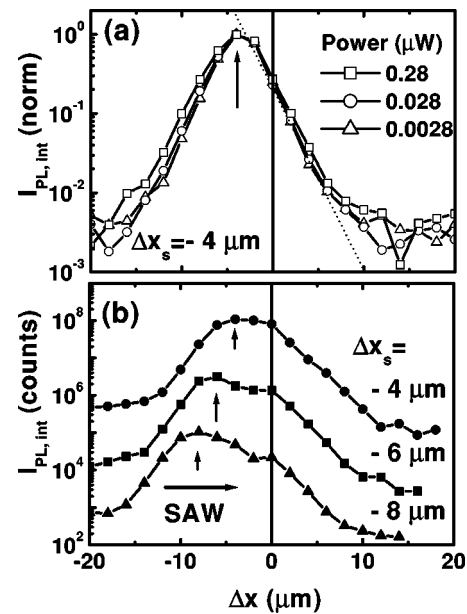


FIG. 3. Spatial dependence of the integrated PL intensity,  $I_{PL,int}$ , detected near the luminescence site  $P_1$  (located at  $\Delta x=0$ ) (a) in the absence and (b) in the presence of a SAW, for different positions  $\Delta x_s$  of the generation spot (indicated by the arrows, the curves were shifted vertically for clarity). The curves in (a), which were recorded for different excitation powers, are normalized to the maximum values. The dotted line in (a) is an exponential fit to the data.

that the recombination energy is close to that of the localized exciton.

Figures 3(a) and 3(b) display PL intensity profiles recorded for excitation at different distances  $\Delta x_s$  from the LS  $P_1$  in the absence and in the presence of a SAW, respectively. The LS is located at the abscissa  $\Delta x=0$  in Figs. 3(a) and 3(b). Under a SAW, the LS appears as a shoulder in the PL profiles of Fig. 3(b), which does not shift with the position of the generation spot.

A further interesting property of the LSs is that, while they act as efficient recombination sites for  $e$  and  $h$  during the ambipolar transport by a SAW, they have a minor effect on the normal exciton diffusion in the absence of a SAW. This behavior is illustrated by the exciton diffusion profiles of Fig. 3(a). For all excitation powers investigated, the integrated PL intensity decays exponentially away from the generation spot, as expected for isotropic diffusion in a two-dimensional system. The PL decay length yields an exciton diffusion length of  $2\mu\text{m}$ . Apparently, the LS does not

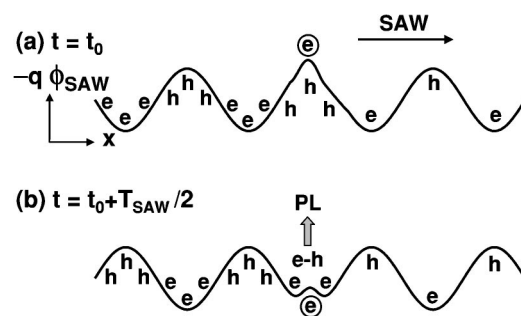


FIG. 4. Potential energy  $-q\Phi_{SAW}$  near a luminescence site for different times  $t$ .  $e$  and  $h$  denote, respectively, electrons and holes transported by the SAW, and  $T_{SAW}$  is the SAW period. The circles indicate charged defects.

modify the diffusion profiles, which remain symmetric on both sides of the generation area.

We attribute the LSs in Fig. 2(b) to the indirect action of charged defects on the carriers transported by the SAW. The electric field produced by the charged defects reduces the magnitude of the transport field acting on the carriers below the value  $F_{\min} = v_{\text{SAW}}/\mu$  ( $\mu$  denotes the carrier mobility) necessary for SAW-induced transport. Due to their lower mobilities, holes are more susceptible of being trapped near a negative defect. During one half of the SAW cycle, positive carriers will accumulate in the QW region close to the defect, as illustrated in Fig. 4(a) [the defects are assumed to be negatively charged in Fig. 4(a)]. In the second half of the SAW period, they will then recombine with carriers of opposite sign transported by the SAW [Fig. 4(b)].

Since the electric field produced by the charged defect must be comparable to the SAW piezoelectric field (of a few kV/cm), the distance between the defects (assumed to have an elementary charge) and the QW must be less than  $0.1 \mu\text{m}$ . From the LS areal density of  $10^6 - 10^7 \text{ cm}^{-2}$  in Fig. 2(b), we calculate an effective volume density of  $10^{11} - 10^{12} \text{ cm}^{-3}$ . The former is considerably higher than the expected density of dislocations, but significantly lower than that of typical interface point defects in (Al,Ga)As/GaAs QWs.<sup>10</sup>

Finally, we briefly consider two types of charged defects which can account for the different impacts of the LCs on exciton diffusion and on the SAW-induced ambipolar transport of  $e$  and  $h$ . The first consists of defects close to the interfaces between the  $\text{Al}_{0.3}\text{Ga}_{0.7}\text{As}$  barrier and the GaAs QW, which are known to act as electron traps.<sup>10,11</sup> In order not to affect the excitons, the defects should only be able to trap electrons and become charged at the locations of high electronic density close to the maxima of the piezoelectric potential. After that, they should remain charged for times considerably larger than the SAW period  $T_{\text{SAW}}$ .<sup>7</sup> The second type of defects are charged sites in the barriers separated

from the GaAs QW plane by a distance  $d$  much larger than the exciton Bohr radius ( $a_B$ ), but considerably shorter than the SAW wavelength. Under these conditions, the electric potential  $\phi_d$  generated by the defect in the QW plane will exert only a small force on excitons [proportional to  $\nabla(\nabla\phi_d \cdot \mathbf{p})$ , where  $\mathbf{p}$  denotes the exciton dipole moment], but will strongly affect the SAW-induced transport of positive and negative charges, which are separated from each other by a distance  $\lambda_{\text{SAW}}/2 \gg a_B$ .

In summary, we have demonstrated that the efficiency of the ambipolar transport of carriers by a SAW in GaAs QWs is limited by radiative recombination sites. These sites, which have different effects on the SAW-induced transport and on the normal exciton diffusion, are attributed to charged defects located in the QW or in the QW barriers.

The authors thank P. Krispin for discussions and for a careful reading of the manuscript. Partial support from the Deutsche Forschungsgemeinschaft, DFG (Project No. SA598/2-1) is gratefully acknowledged.

<sup>1</sup>D. Royer and E. Dieulesaint, *Elastic Waves in Solids* (Springer, Heidelberg, 2000).

<sup>2</sup>M. J. Hoskins and B. J. Hunsinger, *J. Appl. Phys.* **52**, 413 (1984).

<sup>3</sup>F. C. Jain and K. K. Bhattacharjee, *Proc. SPIE* **1347**, 614 (1990).

<sup>4</sup>J. M. Shilton, V. I. Talzyskii, M. Pepper, D. A. Ritchie, J. E. F. Frost, C. J. B. Ford, C. G. Smith, and G. A. C. Jones, *J. Phys.: Condens. Matter* **8**, L531 (1996).

<sup>5</sup>C. Roche, S. Zimmermann, A. Wixforth, J. P. Kotthaus, G. Böhm, and G. Weimann, *Phys. Rev. Lett.* **78**, 4099 (1997).

<sup>6</sup>N. J. Moll, O. W. Otto, and C. F. Quate, *J. Phys. Colloq.* **33**, 231 (1972).

<sup>7</sup>A. Abbate, K. J. Han, I. V. Ostrovskii, and P. Das, *Solid-State Electron.* **36**, 697 (1993).

<sup>8</sup>K. S. Zhuravlev, D. P. Petrov, Yu. B. Bolkhovityanov, and N. S. Rudaja, *Appl. Phys. Lett.* **70**, 3389 (1997).

<sup>9</sup>T. Sogawa, P. V. Santos, S. K. Zhang, S. Eshlaghi, A. D. Wieck, and K. H. Ploog, *Phys. Rev. B* **63**, 121307(R) (2001).

<sup>10</sup>P. Krispin, R. Hey, and H. Kostial, *J. Appl. Phys.* **77**, 5773 (1995).

<sup>11</sup>S. R. McAfee, D. V. Lang, and W. T. Tang, *Appl. Phys. Lett.* **40**, 520 (1982).